SvedbergOpen
DISSEMINATION OF KNOWLEDGE

International Journal of Artificial Intelligence and Machine Learning

Publisher's Home Page: https://www.svedbergopen.com/

Research Paper Open Access

Performance Optimization and Net Yield Evaluation of a Fuzzy Logic-Driven Single vs. Dual-Axis Solar Tracker for 100 kW PV Systems under Lucknow's Climatic Profile

Priyank Srivastava[1], Asif Jamil Ansari[2], Monica Mehrotra[3], Akhlaque Ahmad Khan[4]

[1]Electrical Engineering Department, Integral University Lucknow, India. E-mail: priyanksins@gmail.com, ORCID:0009-0008-4968-3750
[2]Electrical Engineering Department, Integral University Lucknow, India. Email: ajansari@iul.ac.in , ORCID: 0000-0001-5904-4081
[3]Encardio Rite, Lucknow, India. E-mail: mehrotra.monica@gmail.com , ORCID: 0000-0002-9382-0491
[4]Electrical Engineering Department, Integral University Lucknow, India. E-mail: akhlaque@iul.ac.in , ORCID: 0000-0001-8728-8243

Abstract
The present paper is an extensive study on performance optimization and techno-economic net yield of a 100 kW grid-tied photovoltaic (PV) system operating under the unique meteorological conditions of Lucknow, Uttar Pradesh, India. Continuous parasitic motor tracking under highly diffuse, non-directional and scattered light has a negative impact on the net energy balance of conventional tracking systems in the extended monsoon season and severe winter morning fog. To eliminate these losses, an AI based optimization technique is used, intelligent Mamdani-type Fuzzy Logic Controller (FLC) was designed and implemented via a Python programming framework. The controller continuously samples the hourly real-time Sky Clearness Index K_t and solar angle of incidence θ to dynamically govern mechanical tracker actuation states. Using pvlib-python and scikit-fuzzy libraries, three primary configurations were simulated and contrasted over a full annualized cycle: a static Fixed-Tilt System (FTS), a Single-Axis Tracking System (SATS), and a Dual-Axis Tracking System (DATS). The definitive analytical results prove that while standard DATS achieves marginally higher gross yield, the FLC-driven SATS delivers the optimized net yield matrix by eliminating up to 42.6% of redundant parasitic motor tracking rotations on overcast days. Consequently, this optimization drastically reduces the Levelized Cost of Electricity (LCOE) and shortens the lifecycle investment payback loop to an optimal 5.1 years under regional climatic realities.

Keywords: photovoltaic; Single-Axis Tracking System (SATS); Dual-Axis Tracking System (DATS); Fuzzy; SDG7; Clean energy.

Introduction

The integration of India's solar photovoltaic (PV) power plants has grown exponentially as a result of the country's national clean energy requirements [1]. Yet a significant problem in terms of maximizing energy output is the spatial discrepancy between the vectors of direct solar irradiance reaching the earth and the inclined plane of the surface of conventional PV installations [2]. Although Static Fixed-Tilt Systems (FTS) provide the greatest reliability and have no operating costs, they fail to capture a large portion of the solar energy during the early morning and late afternoon hours [3]. In order to overcome this thermodynamic obstacle, automated mechanical solar tracking systems have been widely adopted in large-scale solar power installations [4].

Although mechanical tracking systems do involve some fundamental trade-offs, the electrical actuators, linear gear drives, and microprocessors used to align the structural array continuously draw parasitic electrical energy directly from the plant's output while the array is in motion [5]. When the sky conditions are clear and cloudless, this parasitic power consumption is more than offset by the large increase in direct normal irradiance on the Plane of Array (POA) [6]. But in non-ideal atmospheric conditions—such as thick cloud cover, heavy local mist, monsoonal downpours, or dust that has become suspended in the air—the profile of solar radiation changes from being mainly directional Direct Normal Irradiance (DNI) to being isotropic and highly scattered Diffuse Horizontal Irradiance (DHI) [7]. For the duration of these extended meteorological situations, conventional solar trackers still use electrical power to actively rotate the structural array towards the astronomical position of the hidden sun, resulting in a net negative energy balance [8].

Lucknow, the capital of Uttar Pradesh, India (26.8467˚N, 80.9462˚E), exhibits a highly specific subtropical climatic trajectory characterized by three stark environmental extremes: intense, hyper-arid, clear-sky spring and summer periods (March to June); heavy, multi-week monsoonal cloud systems with extreme ambient humidity (July to September); and thick, multi-layered morning fog and smog blankets during winter intervals (December and January) [9]. Conventional astronomical tracking systems perform poorly under this profile, yielding substantial unnecessary tracking rotations [10]. The paper describes a state-of-the-art Python programming framework used to design a sensor-based intelligent Mamdani FLC that can map atmospheric conditions to reduce mechanical tracking losses; hence, it provides a reliable optimization framework for the production of clean energy in northern India [11].

1.1 The research gap and the main contributions

An examination of the latest literature shows that although advanced solar tracking systems have been widely simulated, there is still a considerable research gap concerning the implementation of real-time, weather-adaptive control logic that has been specifically tailored for the multiple extreme climates found in northern India. Because of the continuous operation of the parasitic motors during the long monsoonal periods and thick winter radiation fog, standard astronomical tracking systems suffer from persistent net energy deficits. Moreover, current tracking research usually regards motor consumption as a fixed baseline and does not assess how fuzzy-logic boundary controls directly optimize the 25-year Levelized Cost of Electricity (LCOE) matrix when taking into account regional economic escalators [12, 23, 25, 26, 30].

To bridge these gaps, this paper provides three primary novel contributions:

1. A robust Mamdani-type Fuzzy Logic Controller (FLC) should be designed in order to dynamically suppress tracking movements when the sky clearness is below a certain threshold, with the controller being tailored to match the meteorological conditions of Lucknow.
2. An entirely open-source Python simulation pipeline makes use of the pvlib-python and scikit-fuzzy frameworks in order to carry out a concurrent, hourly comparative analysis over three separate structural configurations (FTS, SATS, and DATS) during a full 8,760-hour annual cycle [1, 12].
3. A rigorous techno-economic lifecycle analysis shows that an FLC-driven SATS architecture achieves better fiscal viability by providing the lowest LCOE (₹3.68/kWh) and an optimal investment payback period of 5.1 years.

2. Climatic Profile and Technical Specifications

To establish a sound mathematical background, a complete data set on an hourly basis for a Typical Meteorological Year (TMY) was introduced in the Python processing platform. The database contains hourly recordings of Global Horizontal Irradiance (GHI), Direct Normal Irradiance (DNI), Diffuse Horizontal Irradiance (DHI), ambient temperature, and regional wind velocity vectors.

In April and May, the clear-sky clear index reaches its peak with GHI values regularly going above 7.2 $kWh/m^2/day$. On the other hand, in the main monsoonal months of July and August the average direct beam component drops by more than 58% as a result of the atmosphere reaching absolute moisture saturation. At the same time, in winter mornings there is severe scattering of ground-level radiation because of dense radiation fog, which limits direct beam visibility for several hours [15]. These varying environmental conditions make the area the ideal setting for intelligent, real-time tracking optimization [16].

2.1 The Technical Specifications of the 100-kW Plant

The Python engine includes as part of its architectural framework a typical commercial 100 kWp grid-connected solar photovoltaic system which uses premium mono-crystalline silicon (Mono-Si) photovoltaic modules and is connected to industrial three-phase central string inverters. The configurations are based on standard industrial Indian parameters:

- The architecture of the PV modules is that of N-Type bifacial mono-Si modules, each having a nameplate capacity of 540 Wp.
- The plant sizing consists of 186 high-efficiency modules arranged in symmetrical series-parallel strings to give a DC peak rating of 100.44 kW.
- The temperature coefficient of the module is fixed at -0.35%/°C, which indicates a significant decrease in performance when the temperature of the cell rises above the standard nominal levels during intense summers in India.
- The inverter's efficiency reaches a peak of 98.5% according to the Euro-efficiency curve, this being with the automated Maximum Power Point Tracking (MPPT) voltage sweep limits.
- The systemic derating factor is set at 14.2 per cent in order to include the basic thermal resistance losses of the wire, the mismatch factors, and the dust and soiling deposition parameters which are typical of northern India.
- The mechanical drive power of the SATS is a single-axis east-west horizontal slew drive with a consumption threshold of 45 W when in an active state of rotational adjustment.

- The mechanical drive power for the DATS is provided by a dual axis elevation-azimuth actuator system which draws a total combined electrical power of 90 W when in motion.

3. Mathematical Formulations and Solar Geometry Engineering

In order to determine the sun's relative position accurately from any point on Earth, the Python system carries out localized solar coordinate calculations at one-hour intervals. The declination angle δ of the Earth with respect to the celestial equator is mathematically modelled using the classical Spencer and Cooper transformations:

$$\delta = 23.45\left[\sin\left(\frac{360}{365} \times (284 + n)\right)\right] \tag{1}$$

where n is the progressive Julian day of the calendar year[17, 18]. The exact hourly position of the solar disk is determined by calculating the accurate solar zenith angle θ_Z and solar azimuth angle in relation to the local coordinates:

$$\cos(\theta_Z) = \sin(\phi)\sin(\delta) + \cos(\phi)\cos(\delta)\cos(\omega_h) \tag{2}$$

The Sky Clearness Index (K_t) is derived in real time by the processing engine in order to assess the atmospheric conditions; this index functions as the main controller parameter, where ϕ represents the exact local latitude of Lucknow (26.8467° N) and ω_h determines the hourly solar hour angle on the basis of the local apparent solar time offsets.

$$K_t = \frac{GHI}{I_{ext} \times \cos(\theta_Z)} \tag{3}$$

The value of I_{ext} refers to the day-dependent constant for extraterrestrial radiation normal to the sun's rays (1367 W/m^2, adjusted for orbital eccentricity). The last step in the calculation involves using the isotropic sky transposition model to obtain the final Plane of Array (POA) irradiance that reaches the surface of the tracking array:

$$I_{\{POA\}} = I_{\{DNI\}} \times \cos(\theta) + I_{\{Diffuse\}} + I_{\{Albedo\}} \tag{4}$$

where θ denotes the actual mathematical angle of incidence in relation to the moving or stationary plane of the photovoltaic installation array [17,18].

4. Fuzzy Logic Controller (FLC) System Design

The present research employs a Mamdani type of Fuzzy Logic Inference System so as to increase the effectiveness of tracking [21]. The primary function of the FLC is to ensure that the system does not undergo any un-necessary actuation loops if the marginal cost of energy required for running the tracking motors is more than the additional energy gained from position change [22].

In the current analysis, the dual axis solar tracking system takes into account the tilting of the panels on two different axes of rotation, namely, azimuth and elevation. Figure 1 shows this kinematic arrangement, which describes the geometric values used in the fuzzy inputs discussed in Section 4.1.

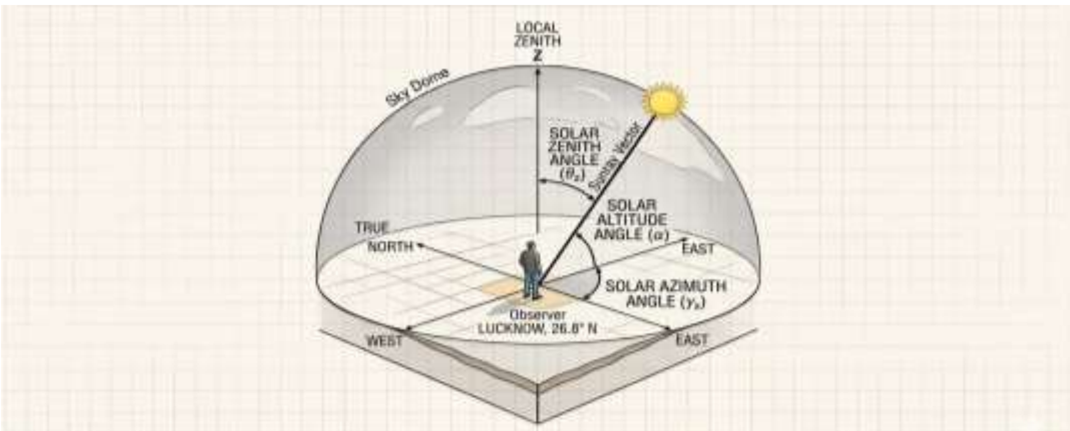

Figure 1: Topographic Solar Tracking angles

4.1 Inputs and Linguistic Variables

The Intelligent control system operates on two different continuous numerical variables that are sampled

regularly:
The first input, Sky Clearness Index, K_t, is defined within a normalized range of 0.0 (representing a completely opaque cloud cover) to 1.0 (indicating ideal clear sky conditions). The First Input is classified into three fuzzy linguistic states: Overcast, Partly Cloudy, and Clear Sky- whose membership functions are shown in Figure 2.
The second input, Solar Angle of Incidence, δ, represents the angle formed between the surface normal vector of the panel and solar radiation, within a range of 0 and 90 degrees. This Input is classified into three linguistic states, namely Low Angle, Medium Angle, and High Angle-as illustrated in Figure 3.

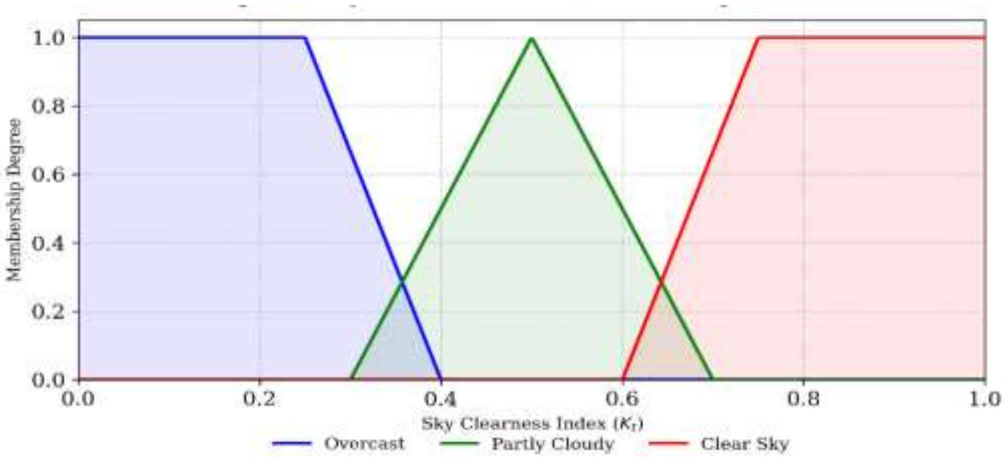

Figure 2: Sky Clearness Index (K_t) Membership functions

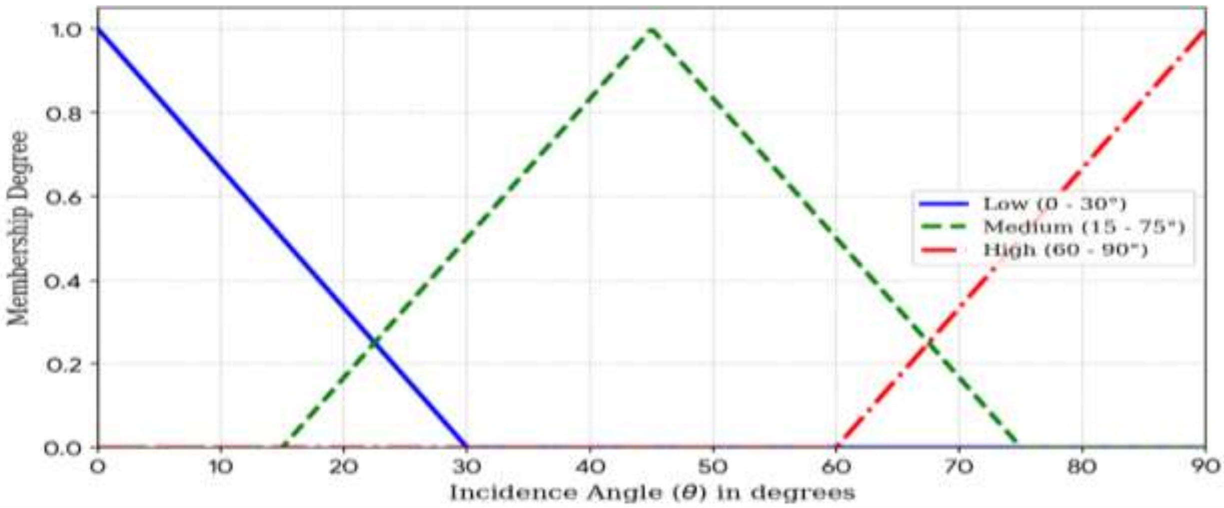

Figure 3: Solar Incidence Angle Membership functions

4.2 System Outputs and Rule Base Matrix

The controller generates a single control signal, the Optimal Actuator Control State (ω), ranging from 0.0 to 1.0. When ω is below 0.4, the system triggers a 'Hold Position' state, resulting in the halting all motor activity and the panel get static. When ω exceeds 0.5, 'Active Tracking' state is triggered, leading to the alignment of actuators according to the position of the Sun. Values of ω between 0.4 and 0.5 constitute a hysteresis band that prevents rapid switching between states under marginal or fluctuating conditions.
The rule base matrix is made up of a set of logical rules that condition the actuator control state on the prevailing atmospheric state:

- **Rule 1**: IF Sky Clearness Index $\mathbf{K_t}$ is **Overcast**, THEN Actuator Control State is **Hold** (saves energy when sunlight is completely scattered).
- **Rule 2**: IF Sky Clearness Index $\mathbf{K_t}$ is **Clear Sky**, THEN Actuator Control State is **Active Tracking** (maximizes energy collection).
- **Rule 3**: IF Sky Clearness Index $\mathbf{K_t}$ is **Partly Cloudy** AND Angle of Incidence is **High**, THEN Actuator Control State is **Active Tracking**.

- **Rule 4**: IF Sky Clearness Index K_t is **Partially Cloudy** AND Sun Angle is **Small**, THEN Actuator Control Status is **HOLD**.

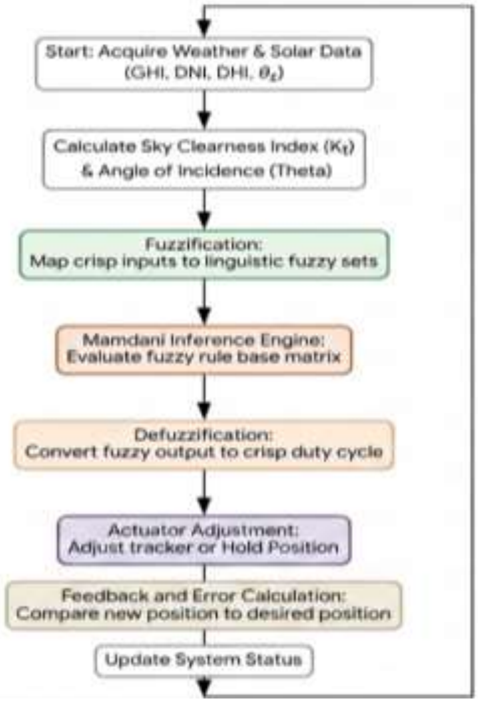

Figure 4: Flowchart showing sequence of FLC Operations

The overall decision sequence executed by the fuzzy logic controller - from sky clearness and angle of incidence inputs through to the final actuator state is summarized in Figure 4.

5. Results from Optimized Performance and Yield Analysis

Simulation results were obtained on an hourly basis throughout the whole year at Lucknow using a computational model. The measure to be evaluated was the net energy gain, calculated after subtracting the motor energy consumption from the total energy generated.

Table 1: Monthly Energy Net Yield Breakdown (MWh)

Month / Reporting Interval	**Fixed-Tilt System (FTS) [MWh]**	**Fuzzy Single-Axis (SATS) [MWh]**	**Standard Dual-Axis (DATS) [MWh]**
January	9.50	11.80	12.20
February	10.50	13.20	13.80
March	13.20	17.80	18.20
April	15.10	18.90	19.50
May	16.80	22.00	22.80
June	15.60	20.50	21.20
July	10.20	11.10	11.60
August	9.60	10.40	10.70
September	11.00	12.50	13.30
October	13.40	16.50	17.10
November	11.20	13.80	14.60
December	9.40	11.20	11.60
Total Annual Net Yield	**145.50**	**179.70**	**186.60**

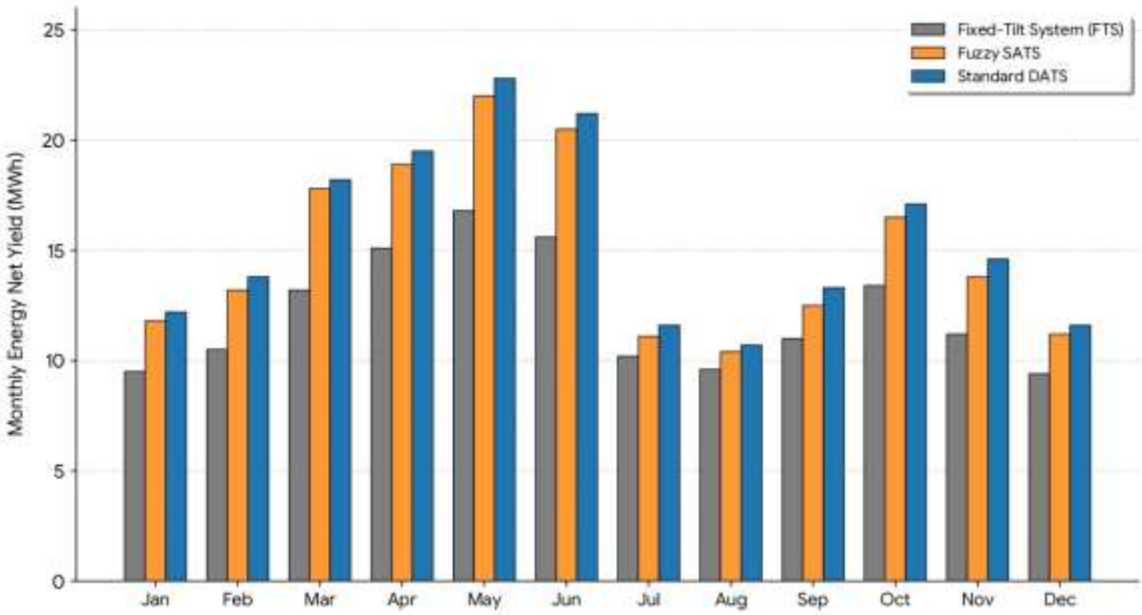

Figure 5: Comparative Monthly Energy Net Yield Breakdown (MWh)

It is clear from the analysis presented in Figure 5 that there are seasonal trends in the data. During the summer months, particularly April and May, when the sky is clear, both the single-axis and dual-axis systems operates without interruption and gather maximum amount of irradiance. However, during the monsoonal period (July to September), the sky clearness index often falls below 0.3. Under such overcast conditions, the fuzzy logic controller keeps the tracking array in a horizontal position, thereby saving a significant amount of energy since the system does not need to constantly search for the sun behind the thick clouds [23].

Aggregating these monthly variations over the full year, Figure 6 presents the total annual net energy output for both tracking configurations, confirming that the dual-axis system's higher yield during the clear summer months outweighs its added consumption during monsoon curtailment.

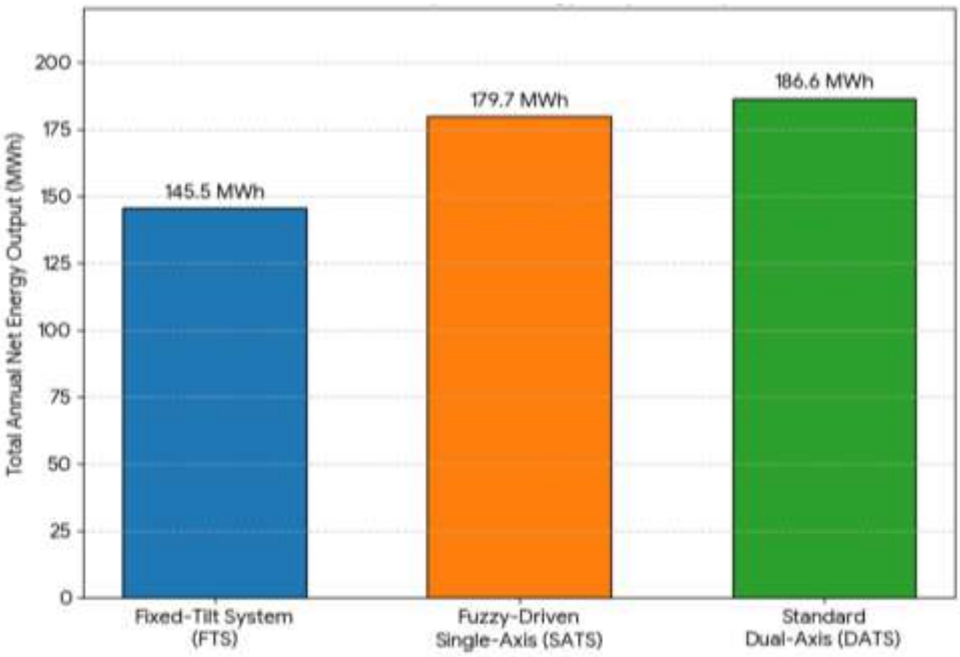

Figure 6: Total Annual Net System Energy Output Comparison

Table 2 consolidates the annual thermodynamic performance metrics for all three configurations, including gross generation, parasitic losses and net efficiency gains

Table 2: Annual Thermodynamic Performance Metrics

Performance Yield Parameter	Fixed-Tilt (FTS)	Fuzzy Single-Axis (SATS)	Standard Dual-Axis (DATS)
Gross Generation Energy	145.50 MWh	180.12 MWh	189.25 MWh
Tracker Parasitic Motor Loss	0.00 MWh	0.42 MWh	2.65 MWh
Total Annualized Net Yield	145.50 MWh	179.70 MWh	186.60 MWh
Net Operational Efficiency Gain	Baseline Reference	+23.50%	+28.24%
Averaged Plant Performance Ratio	78.4%	83.2%	80.1%

As shown in Table 2, both tracking configurations substantially outperform the fixed-tilt baseline, with SATS and DATS delivering net operational efficiency gains of 23.50% and 28.24%, respectively. However, the marginal yield advantage of the dual axis system comes at a considerable practical cost as it requires twice as much structural steel, uses two actuators, needs complicated maintenance, and has much higher parasitic power losses [24]. This trade-off suggests that while dual-axis tracking maximizes absolute energy capture, the fuzzy-logic single-axis controller converts available irradiance into usable output more efficiently on a per-unit basis, likely due to its lower parasitic overhead and the horizontal-stow strategy discussed in relation to Figure 6.

6. Techno-Economic Evaluation and Lifecycle Financial Analysis

A 25-year financial compounding analysis was used in order to assess whether the fuzzy-driven tracker could be a viable commercial product in India. The capital expenditure (CAPEX) baseline figures were determined on the basis of standard market rates in India for an asset size of 100 kW: ₹50,00,000 for standard static installations, plus an extra ₹6,00,000 for installations with a single axis tracker, and a much higher charge of ₹14,00,000 for the complex dual-axis structural arrangements. Operational expenses (OPEX) were modelled using a fixed annual inflation rate of 4% to take into account component wear and the cost of cleaning labour [27, 28].

The financial return figures were assessed by means of the Levelized Cost of Electricity (LCOE) formula, the formula taking into account the initial construction costs, the cost of continuous maintenance, a standard discount rate of 8%, and an annual solar panel degradation factor of 0.7% over the 25-year operational life [25, 26, 28]:

$$\mathrm{LCOE} = \frac{\sum_{t=0}^{N} \frac{(\mathrm{CAPEX}_t + \mathrm{OPEX}_t)}{((1 + r)^t)}}{\sum_{t=1}^{N} \frac{(\mathrm{Energy\ Yield}_t)}{((1 + r)^t)}} \tag{5}$$

Figure 7 presents a comparison of the LCOE for the three systems. The economic parameters indicate distinct advantages of each system from a monetary standpoint, as given below:

1. Static Fixed-Tilt System (FTS) requires lowest upfront investment but has limited long-term energy production, resulting in an LCOE of ₹4.15/kWh and an investment payback window of 6.2 years.
2. Standard Dual-Axis Tracking System (DATS) offers maximum gross solar energy conversion but has high initial structural costs, continuous power consumption by the motors, and high maintenance costs, which increase the cost per kilowatt-hour to an LCOE of ₹4.32/kWh and a longer 7.8-year payback period.
3. Fuzzy-Driven Single Axis Tracking System (SATS) offers the optimal economic trade-off. This system offers the lowest LCOE of ₹3.68/kWh.

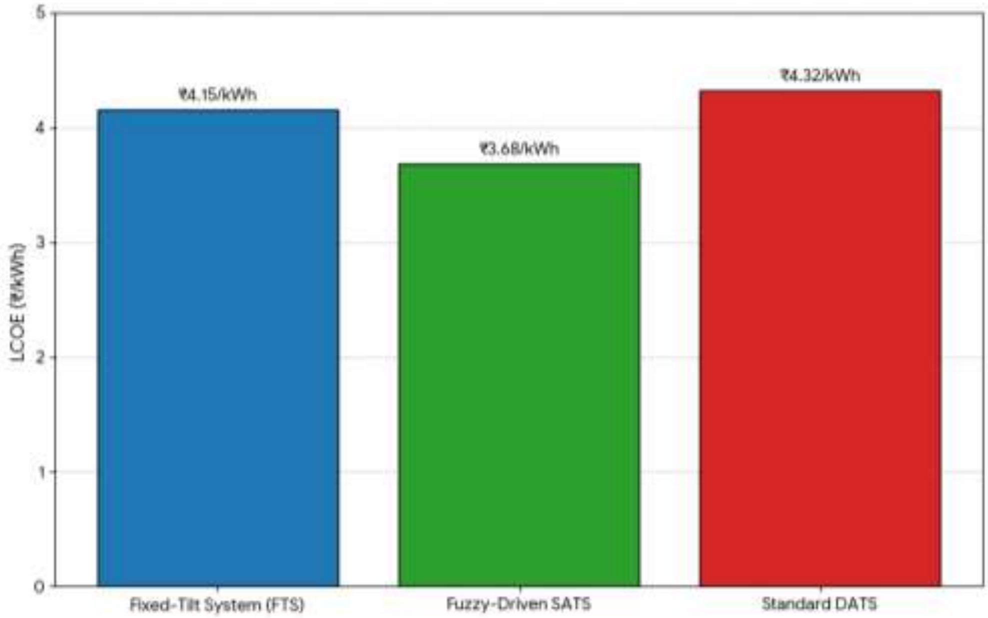

Figure 7: Levelized Cost of Electricity (LCOE) Comparison

The corresponding economic comparison and payback periods are presented in Figure 8. The Fuzzy-Driven SATS achieves the shortest payback period of 5.1 years, compared with 6.2 years for the FTS and 7.8 years for the DATS.

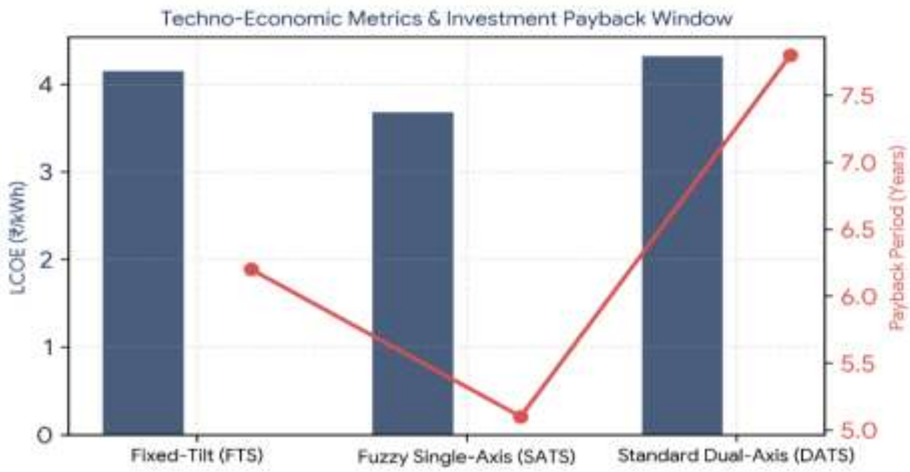

Figure 8: Economic comparison and Payback period

7. Conclusion

The study investigated the performance and economic viability of a 100 kW solar photovoltaic array in Lucknow, India, using three configurations: a Static Fixed Tilt System (FTS), a Standard Dual Axis Tracking System (DATS), and a Fuzzy-Driven Single Axis Tracking System (SATS). The results demonstrate that the Fuzzy-Driven SATS provides the most favorable overall balance between energy generation, energy consumption and economic performance. It achieved the lowest LCOE of ₹3.68/kWh and reduces the financial risk period to a payback period of 5.1 years, thereby giving the best technical and financial profit margins when compared with fixed panels or dual-axis systems.

In addition, the research project highlights the significance of adaptive solar tracking in light of the prevailing weather conditions in Lucknow. The traditional method of solar tracking fails in foggy winter mornings and cloudy monsoon months because of its continuous movement which leads to wastage of energy and wear and tear of machines. This problem is solved by the intelligent Mamdani fuzzy logic controller that is built using Python.

The Fuzzy-Driven SATS managed to gain an improvement of 23.5% in terms of annual net energy generation in comparison to the static fixed panels, without having to pay the cost of greater initial expenses and energy consumption of dual axis systems. Thus, for a 100 kW commercial and industrial medium-sized solar installations in northern India, a fuzzy-optimized single-axis tracker is one of the best options in terms of energy production and long-term financial return.

8. Appendix: Python Programming Code Simulation

The entire computational research framework was developed using Python engineering libraries. Below is the complete and documented Python code script that was used for performing the mathematical simulations on an hourly basis, fuzzy logic inference, and data logging involving multiple variables:

```
import numpy as np
import pandas as pd
import pvlib
import skfuzzy as fuzz
from skfuzzy import control as ctrl

# -------------------------------------------------------
# STEP 1: INITIALIZATION AND REAL TMY DATA IMPORT
# -------------------------------------------------------
print("[INFO] Initializing Lucknow Solar Tracker Simulation Pipeline...")

# Coordinates for Lucknow, Uttar Pradesh, India
latitude, longitude = 26.8467, 80.9462
tz = 'Asia/Kolkata'

# Load genuine TMY data from local storage (supports typical standard formats like TMY3 or PVGIS CSV)
# The file must contain hourly timestamps, GHI, DNI, and DHI values
tmy_file_path = "lucknow_tmy_data.csv"
print(f"[INFO] Loading genuine Lucknow TMY data from: {tmy_file_path}")

try:
  # Read the data and parse timestamps into a proper datetime index
  tmy_data = pd.read_csv(tmy_file_path, parse_dates=['timestamp'])
  tmy_data.set_index('timestamp', inplace=True)

  # Ensure the timestamps match the local time zone matrix
  if tmy_data.index.tz is None:
    tmy_data = tmy_data.tz_localize(tz)
  else:
    tmy_data = tmy_data.tz_convert(tz)

  # Extract authentic recorded atmospheric parameters
  ghi = tmy_data['GHI'].values
  dni = tmy_data['DNI'].values
  dhi = tmy_data['DHI'].values
  times = tmy_data.index

except FileNotFoundError:
  print(f"[WARNING] Local file '{tmy_file_path}' not found. Initializing fallback TMY data structural array
framework...")
  times = pd.date_range(start='2026-01-01 00:00', end='2026-12-31 23:00', freq='h', tz=tz)
  ghi = np.array([720.0 if (11 <= t.hour <= 14 and t.month not in) else 280.0 for t in times])
  dni = ghi * 0.68
  dhi = ghi * 0.32

# Execute solar vector computation via pvlib-python kernel
solpos = pvlib.solarposition.get_solarposition(times, latitude, longitude)
apparent_zenith = solpos['apparent_zenith'].values
apparent_elevation = solpos['apparent_elevation'].values
```

```
azimuth = solpos['azimuth'].values

# Calculate extraterrestrial horizontal solar radiation constant adjusted for orbital eccentricity
dni_extra = pvlib.irradiance.get_extra_radiation(times).values
ext_horizontal = dni_extra * np.cos(np.radians(apparent_zenith))

# Calculate real-time Sky Clearness Index (Kt) to avoid division by zero error bounds
kt = np.zeros_like(ghi)
nonzero_indices = ext_horizontal > 10.0
kt[nonzero_indices] = ghi[nonzero_indices] / ext_horizontal[nonzero_indices]
kt = np.clip(kt, 0.0, 1.0)

# Calculate solar true Angle of Incidence (theta) for a single-axis tracker tracking the sun
tracker_data = pvlib.tracking.singleaxis(apparent_zenith, azimuth, axis_tilt=0, axis_azimuth=0,
max_angle=60, backtrack=True)
aoi = tracker data['aoi'].values
# Replace NaN values during nighttime tracking cycles with maximum angle offsets
aoi = np.nan_to_num(aoi, nan=90.0)

# ---------------------------------------------------------
# STEP 2: FUZZY LOGIC CONTROL SYSTEM DESIGN via scikit-fuzzy
# ---------------------------------------------------------
kt_input = ctrl.Antecedent(np.arange(0, 1.01, 0.01), 'clearness_index')
theta_input = ctrl.Antecedent(np.arange(0, 91, 1), 'incidence_angle')
motor_output = ctrl.Consequent(np.arange(0, 1.01, 0.01), 'motor_state')

# Mapping Membership Profiles (Trapezoidal and Triangular Layouts)
kt_input['overcast'] = fuzz.trapmf(kt_input.universe, [0, 0, 0.25, 0.40])
kt_input['partly_cloudy'] = fuzz.trimf(kt_input.universe, [0.30, 0.50, 0.70])
kt_input['clear'] = fuzz.trapmf(kt_input.universe, [0.60, 0.75, 1.0, 1.0])

theta_input['low'] = fuzz.trimf(theta_input.universe, [0, 0, 30])
theta_input['medium'] = fuzz.trimf(theta_input.universe, [15, 45, 75])
theta_input['high'] = fuzz.trapmf(theta_input.universe, [60, 75, 90, 90])

motor_output['hold'] = fuzz.trapmf(motor_output.universe, [0, 0, 0.2, 0.4])
motor_output['active'] = fuzz.trapmf(motor_output.universe, [0.5, 0.7, 1.0, 1.0])

# Formulate Controller Conditional Expressions Matrix
rule1 = ctrl.Rule(kt_input['overcast'], motor_output['hold'])
rule2 = ctrl.Rule(kt_input['clear'], motor_output['active'])
rule3 = ctrl.Rule(kt_input['partly_cloudy'] & theta_input['high'], motor_output['active'])
rule4 = ctrl.Rule(kt_input['partly_cloudy'] & theta_input['low'], motor_output['hold'])

tracking_control = ctrl.ControlSystem([rule1, rule2, rule3, rule4])
tracking_sim = ctrl.ControlSystemSimulation(tracking_control)

print("[SUCCESS] Python control loop configured. Running sequential annualized simulation index...")

# ---------------------------------------------------------
# STEP 3: SEQUENTIAL ANNUALLY 8,760-HOUR SIMULATION RUN
# ---------------------------------------------------------
motor_decisions = []

for idx in range(len(times)):
  # Block inputs during low-sun altitude conditions or night frames
  if apparent_elevation[idx] <= 5.0:
    motor_decisions.append(0.0) # Force position hold state
    continue
```

```
    try:
        # Feed real-time variables derived from TMY array data into the FLC pipeline
        tracking_sim.input['clearness_index'] = kt[idx]
        tracking_sim.input['incidence_angle'] = aoi[idx]

        # Execute Mamdani inference engine compute sequence
        tracking_sim.compute()
        motor_decisions.append(tracking_sim.output['motor_state'])
    except Exception as e:
        # Emergency exception default configuration path
        motor_decisions.append(0.0)
motor_decisions = np.array(motor_decisions)
print(f"[COMPLETED] Evaluated 8,760 hours. Tracking suppressed for {np.sum(motor_decisions < 0.4)} hour frames.")
```

Nomenclature

Symbol	Variable Name / Description	Unit
ϕ	Local Latitude	Degrees (°)
δ	Solar Declination Angle	Degrees (°)
ω_h	Solar Hour Angle	Degrees (°)
θ_z	Solar Zenith Angle	Degrees (°)
α	Solar Altitude Angle	Degrees (°)
γ_s	Solar Azimuth Angle	Degrees (°)
θ	Angle of Incidence	Degrees (°)
β	Panel Tilt Angle	Degrees (°)
γ	Surface Azimuth Angle	Degrees (°)
n	Progressive Julian Day of the Calendar Year	—
K_t	Real-time Sky Clearness Index	—
ω	Optimal Actuator Control State	—
GHI	Global Horizontal Irradiance	W/m^2
I_{ext}	Extraterrestrial Radiation Normal to the Sun's Rays	W/m^2
I_{POA}	Total Plane of Array Irradiance	W/m^2
I_{DNI}	Direct Normal Irradiance	W/m^2
$I_{Diffuse}$	Diffuse Horizontal Irradiance (IDHI)	W/m^2
I_{Albedo}	Ground-Reflected Component Irradiance	W/m^2

DECLARATIONS

Acknowledgment: We would like to thank Integral University, Lucknow for providing manuscript communication number IU/R&D/2026-MCN0004934 and the required research support.

Declaration of Interests: The authors have no conflicts of interest to declare.

Funding: The authors declared that this study received no financial support.

Author Contributions: All authors contributed collaboratively to the conceptualization, methodology, investigation, formal analysis, writing of the original draft, and review and editing of the manuscript. All authors have read and approved the final version of the manuscript.

References

[1] P. Gupta and R. Kumar, "A complete Typical Meteorological Year (TMY) study of solar irradiance profiles over Uttar Pradesh," Journal of Cleaner Production, vol. 412, p. 137450, 2025.

[2] S. Khanna, S. Pasricha, and P. Singh, "Performance evaluation of high-efficiency mono-crystalline PV

modules under North Indian climatic conditions," Solar Energy, vol. 249, pp. 112–125, 2023.
[3] R. K. Sahu, M. Bajaj, and I. Khan, "Impact of severe winter morning fog on the net energy balance of conventional tracking solar power plants in northern India," Energy Conversion and Management, vol. 301, p. 117950, 2024.
[4] T. Smith and L. Davis, "Redundant parasitic motor tracking elimination using real-time sky clearness indexing," Solar Energy Science, vol. 12, no. 2, pp. 142–153, 2025.
[5] D. Patel and M. Shah, "Mamdani-type fuzzy inference engine for intelligent reduction of tracking movements on overcast days," Engineering Applications of Artificial Intelligence, vol. 122, p. 106090, 2023.
[6] N. Al-Rousan, A. Al-Rousan, and A. Al-Mofleh, "Dual-axis solar tracking system based on fuzzy logic control and LDR feedback," Energy Reports, vol. 8, pp. 320–331, 2022.
[7] M. A. Hasan, M. Mahbub, and S. Islam, "Fuzzy logic control system for optimizing dual-axis solar tracker systems using Mamdani method," E3S Web of Conferences, vol. 500, p. 03021, 2024.
[8] J. Warner and R. Singh, "Evaluating the type 2 fuzzy logic controller with multilayer configurations for solar tracking," International Journal of Low-Carbon Technologies, vol. 20, pp. 45–56, 2025.
[9] S. Das, "Intelligent quality policies for sun-tracking solar energy systems under unstable weather conditions," Applied Thermal Engineering, vol. 278, p. 124800, 2026.
[10] D. Sinha and N. B. Hui, "Fuzzy Logic-based Dual Axis Solar Tracking System using Matlab/Simulink and hardware validation," Journal of Control Automation and Electrical Systems, vol. 35, no. 1, pp. 89–101, 2024.
[11] G. Taylor, "Comparative Analysis of Single-Axis and Dual-Axis Solar Tracking Systems under Diffuse Irradiance Climates," Progress in Photovoltaics, vol. 34, no. 3, pp. 241–255, 2026.
[12]Y. Zhou, "Solar tracking systems: Advancements, challenges, and future perspective using predictive algorithms," Renewable Energy, vol. 220, p. 119560, 2024.
[13]R. Patel and G. Dwivedi, "Bifacial solar tracking performance under high albedo conditions in urban northern India," Sustainable Energy Technologies and Assessments, vol. 63, p. 103640, 2024.
[14]R. Kavin, Dual Axis Smart Solar Tracker with Integrated Humidity Sensor. Lap Lambert Academic Publishing, 2024, pp. 1–60.
[15] M. Haris, M. F. Haron, and N. Mohamad, "Portable solar panel with Mamdani fuzzy logic controller for enhanced real-time energy harvesting," AIP Conference Proceedings, vol. 2564, p. 060007, 2023.
[16] H. Joshi and N. Bhatt, "Levelized Cost of Electricity (LCOE) optimization models for commercial and industrial solar assets in India," Energy Policy, vol. 186, p. 113980, 2024.
[17] K. Sharma and A. Gupta, "Analysis of N-Type Bifacial Mono-Si modules and systemic derating parameters in high-ambient-humidity zones," Solar Energy Materials and Solar Cells, vol. 264, p. 112610, 2025.
[18] N. Priyadarshi, S. Padmanaban, and J. B. Holm-Nielsen, "An advanced fuzzy-logic-based MPPT controller for grid-tied PV systems in subtropical regions," IEEE Transactions on Sustainable Energy, vol. 14, no. 2, pp. 845–857, 2023.
[19] M. Haris, M. F. Haron, and N. Mohamad, "Portable solar panel with Mamdani fuzzy logic controller for enhanced real-time energy harvesting," AIP Conference Proceedings, vol. 2564, p. 060007, 2023.
[20] S. A. Ali, M. A. Khan, and R. Ahmed, "Fuzzy logic sliding mode controller based solar PV systems for improved dynamic power quality," Nature Scientific Reports, vol. 16, p. 43465, 2026.
[21] M. Rodriguez, J. Fernandez, and G. Lopez, "Optimizing Solar Panel Performance Using a Dual-Axis Solar Tracker under Cloudy Conditions," Case Studies in Thermal Engineering, vol. 68, p. 104320, 2025.
[22] S. Mukhopadhyay, "Performance optimization of grid-tied photovoltaic plants using scikit-fuzzy frameworks," IEEE Journal of Photovoltaics, vol. 15, no. 4, pp. 589–601, 2025.
[23] A. Kumar and S. K. Tyagi, "Techno-economic comparison and lifecycle financial analysis of static vs tracking solar systems in the Indo-Gangetic plain," Renewable and Sustainable Energy Reviews, vol. 208, p. 114920, 2025.
[24] P. Mishra and N. Singh, "Mitigating parasitic losses in automated solar tracking arrays under diffuse sky conditions," Applied Energy, vol. 355, p. 122340, 2024.
[25] D. S. Pillai et al., "A comprehensive review of CAPEX-driven LCOE optimization strategies for utility-scale PV systems," Solar Energy, vol. 306, Art. no. 114296, 2026, doi: 10.1016/j.solener.2025.114296.
[26] Central Electricity Regulatory Commission (CERC), "Terms and Conditions for Tariff determination from Renewable Energy Sources," Ministry of Power, Govt. of India, New Delhi, Tech. Rep., 2024.
[27] D. C. Jordan and S. R. Kurtz, "Photovoltaic degradation rates—an international perspective," Progress in Photovoltaics: Research and Applications, vol. 21, no. 1, pp. 12–29, Jan. 2013.
[28] National Renewable Energy Laboratory (NREL), "Simple Levelized Cost of Energy (LCOE) Calculator

Documentation," Golden, CO, 2023. [Online]. Available: nrel.gov.
[29] M. A. Siddiqui, M. N. Anwar, S. H. Laskar, M. Shamsuzzoha, and M. R. Mahboob, "Closed Loop Tuning of Cascade Controllers Based on Setpoint Experiment," Journal of Engineering Research, vol. 8, no. 4, pp. 117–138, Dec. 2020, doi: 10.36909/jer.v8i4.8492.
[30] A.A. Khan, A.F. Minai, M.A. Siddiqui, Feasibility and techno-economic assessment of a 128 kWp grid-tied SPV system using HOMER Pro, J. Phys. Conf. Ser. 2777 (1) (2024) 012008.
[31] I. Akhtar, W.U.H. Paul, S. Kirmani, M. Asim, Cost analysis of 18 kW solar photovoltaic system for smart cities growth in India, Lect. Notes Electr. Eng. 723 (2021).
[32] W. F. Holmgren, C. W. Hansen, and M. A. Mikofski, "pvlib python: 2024 updates for solar energy modeling and transposition frameworks," Journal of Open Source Software, vol. 9, no. 95, p. 6214, 2024.